

REPORT DOCUMENTATION PAGE			Form Approved OMB No. 0704-0188
<p>Public reporting burden for this collection of information is estimated to average one hour per response, including the time for reviewing instructions, searching existing data sources, gathering and maintaining the data needed, and completing and reviewing the collection of information. Send comments regarding this burden estimate or any other aspect of this collection of information, including suggestions for reducing the burden to Washington Headquarters Services. Directorate for Information Operations and Reports, 1215 Jefferson Davis Highway, Suite 1204, Arlington, VA 22202-4302, and to the Office of Management and Budget, Paperwork Reduction Project (0704-0188), Washington, DC 20503.</p>			
1. AGENCY USE ONLY (Leave blank)	2. REPORT DATE	3. REPORT TYPE AND DATES COVERED	
	7/3/96	Final Technical Report	
4. TITLE AND SUBTITLE		5. FUNDING NUMBERS	
<b>Shelf Circulation in the Gulf of Mexico</b>		ONR N00014-90-J-1127	
6. AUTHOR(S)		8. PERFORMING ORGANIZATION REPORT NUMBER	
Guillermo Gutierrez Velasco Clinton D. Winant			
7. PERFORMING ORGANIZATION NAMES(S) AND ADDRESS(ES)		10. SPONSORING/MONITORING AGENCY REPORT NUMBER	
Center for Coastal Studies Scripps Institution of Oceanography University of California, San Diego La Jolla, CA 92093-0209		19960722 097	
9. SPONSORING/MONITORING AGENCY NAME(S) AND ADDRESS(ES)		11. SUPPLEMENTARY NOTES	
Office of Naval Research Department of the Navy 800 North Quincy Street Arlington, VA 22217-5500			
12a. DISTRIBUTION/AVAILABILITY STATEMENT		12b. DISTRIBUTION CODE	
No restrictions		<div style="border: 1px solid black; padding: 2px; display: inline-block;"> <b>DISTRIBUTION STATEMENT A</b>            Approved for public release            Distribution Unlimited         </div>	
13. ABSTRACT (Maximum 200 words)			
<p>Meteorological observations from an array of stations deployed along the periphery of the Gulf of Mexico between 1990 and 1993, are used to describe the seasonal fluctuations in patterns of atmospheric variables from a contemporary set of measurements. Seasonal maps of wind stress based on these measurements resemble wind stress maps based on ship observations, as published by Elliot (1979), rather than maps based on analyses of numerical weather forecasts, as published by Rhodes et al. (1989), particularly near the western boundary of the Gulf. Seasonal maps of wind stress curl are characterized by positivecurls over the western and southwestern Gulf. The central result of this study is to document the important role of the mountain chain which extends along the southwestern section of the Gulf in channeling the wind towards the isthmus of Tehuantepec.</p>			
14. SUBJECT TERMS		15. NUMBER OF PAGES	
meteorological observations, weather forecasts, wind, wind stress curl		35	
		16. PRICE CODE	
17. SECURITY CLASSIFICATION OF REPORT	18. SECURITY CLASSIFICATION OF THIS PAGE	19. SECURITY CLASSIFICATION OF ABSTRACT	20. LIMITATION OF ABSTRACT
Unclassified	Unclassified	Unclassified	UL

UNIVERSITY OF CALIFORNIA, SAN DIEGO UCSD

---

BERKELEY • DAVIS • IRVINE • LOS ANGELES • RIVERSIDE • SAN DIEGO • SAN FRANCISCO



---

SANTA BARBARA • SANTA CRUZ

CENTER FOR COASTAL STUDIES, 0209  
SCRIPPS INSTITUTION OF OCEANOGRAPHY

9500 GILMAN DRIVE  
LA JOLLA, CALIFORNIA 92093-0218  
PHONE: (619) 534-4333  
FAX: (619) 534-0300

July 9, 1996

Defense Technical Information Center  
Building 5, Cameron Station  
Alexandria, Virginia 22314

Enclosed you will find the requested 4 copies of the Final Technical Report for grant number: ONR NOOO14-90-J-1127 entitled "Shelf Circulation in the Gulf of Mexico." If you have any questions at all please contact Judy Keplinger at (619) 534-3567.

Thank you for your time.

Sincerely,

A handwritten signature in black ink, appearing to read "Judy K." or "Judy Keplinger".

## 1. Introduction

The Gulf of Mexico is located at the transition between the subtropical and tropical climate zones. At mid-latitudes, the strength and position of the high pressure cells fluctuate on seasonal and shorter time scale, affecting the circulation and the air masses present over the continents. This seasonal fluctuation has a profound influence on the climate over the North American continent and over the Gulf of Mexico in particular, resulting in frontal incursions and cold air outbreaks, with increased frequency during the winter. Seasonal variability is less pronounced in the tropics, and temperature gradients are weaker than in the sub-tropics. In this zone, atmospheric variability is primarily due to penetration of extra tropical weather systems and to wave disturbances which propagate in the tropical easterlies, and which can intensify and generate tropical storms and hurricanes.

The momentum flux between the atmosphere and the underlying ocean represents a major motive force for the ocean. Elliott [1979] describes patterns of wind stress over the Gulf of Mexico based on ship observations. Seasonal estimates of wind stress on a one degree grid are used to compute seasonal estimates of the wind stress curl field. In Elliott's maps the wind stress curl varies in sign, a large area of negative curl occupies the northern and eastern portion of the Gulf, while the curl is generally positive over the southwest Gulf.

The spatial and temporal resolution of the patterns derived from ship observations are limited, accordingly estimates of wind stress derived from analyses produced by numerical forecasting centers have been used to provide higher resolution maps. In order to improve the resolution Rhodes et al. [1989] (hereafter RTW) combined surface pressure analyses compiled by the U. S. National Weather Service with meteorological observations from buoys deployed by the National Data Buoy Center (NDBC), notably three buoys deployed along 26 °N. Seasonal patterns of wind stress and wind stress curl estimated

from analyses and station observations differ significantly, both in direction and in magnitude, from the estimates derived from ship observations. The most conspicuous differences occur in the southwest corner of the Gulf where the maps based on ship observations suggest a northerly wind stress, particularly during fall, winter and spring, whereas the maps based on analyses suggest an easterly wind stress in these areas. Wind stress curl distributions are accordingly different: the curl maps based on analyses are all characterized by large negative values near the western boundary, while the maps estimated from ship observations are characterized by a curl of opposite sign in the same area. RTW comment that the differences cannot be resolved due to the lack of an independent data set for comparison.

The sign and amplitude of the wind stress curl over the western Gulf are important in determining the strength and sign of the underlying wind driven ocean circulation. Sturges [1993] uses the maps produced by RTW, based on numerical analyses to conclude that the annual cycle of the flow along the western boundary is driven by the annual variation in the wind stress curl, augmented by Ekman pumping over the western Gulf.

While station observations of several meteorological parameters are routinely available north of the Mexican-US border, continuous observations of meteorological variables from well exposed stations on the periphery of the Gulf are relatively scarce south of the border. The results described here were obtained by combining observations from the array of stations maintained north of the border with observations taken in the course of a cooperative program between Mexico and the U. S. This program deployed and maintained a number of stations at well exposed coastal locations or island sites on the Mexican side of the Gulf for a period of three years. The combined set of observations is used to describe seasonal patterns of air-sea exchange on a Gulf-wide scale.

## 2. The Observations

In August 1990, an array of six meteorological stations were deployed in the southern coast of the Gulf of Mexico for a three year period, in a cooperative project between Mexican and US scientists, at the six locations illustrated in Figure 1. With the exception of Coatzacoalcos, all the stations were located on well exposed islands, away from the mainland. At Coatzacoalcos, the instruments were located atop the building housing the Naval Command, and well exposed to the prevailing wind direction. The actual location of each station is listed in Table 1. Instruments deployed at each station included wind speed and direction sensors, atmospheric pressure and air temperature sensors. The wind speed and direction were monitored with an R.M. Young sensor mounted on a 10 m aluminum mast. Stated accuracy for speed and direction are  $0.1 \text{ m s}^{-1}$  and  $1.5^\circ$  respectively. The barometric pressure was measured with a Paroscientific Digiquartz transducer with an accuracy of 70 Pa. The air temperature was monitored with a YSI thermistor. The overall accuracy of the air temperature measurement was  $0.01^\circ\text{C}$ . All stations were inspected regularly and field calibrations were performed every six months. At each station a temperature sensor was deployed in the water, 1 m beneath the surface. The accuracy of the water temperature sensor was  $0.01^\circ\text{C}$ . All the sensor information was digitized each minute and recorded.

The observations from the array deployed in Mexico were augmented by observations acquired from sixteen stations deployed and maintained by NDBC north of the border, including four buoys deployed in the Gulf. The location of those stations is listed in Table 1 and illustrated in Figure 1. Station SVLS1 observations are included in the analysis although it is outside the area illustrated in Figure 1. The NDBC stations are instrumented to measure winds 10 m above sea level, atmospheric pressure, and air and sea temperature. The accuracy of the wind speed sensor, as reported by Hamilton [1980] is  $1 \text{ m s}^{-1}$  and the

accuracy of the direction sensor is  $10^\circ$ . The accuracy of the barometric sensor is stated to be  $1 \times 10^2$  Pa and the air and sea temperature observations have an accuracy of  $1^\circ\text{C}$ .

The analyses described subsequently were all based on hourly averages of the original measurements. In order to describe fluctuations with periods longer than one day the time series were filtered using a low pass filter with half amplitude at 0.015 cycles per hour (corresponding to a period of 2.78 days). Since wind stress rather than wind speed is responsible for the flux of momentum between the atmosphere and the ocean, winds are converted to wind stress following the method described by Large and Pond [1981] for a neutral atmosphere. While the usual meteorological convention is to indicate the wind direction as that from which it is blowing, the oceanographic convention is to report the direction towards which the wind is flowing. In this paper we adopt the oceanographic convention.

Two options are available to describe the statistics of a vector quantity such as the horizontal wind over some time period. The wind can be described by amplitude (speed) and direction relative to some arbitrary direction, say North, and the means and higher order moments of the speed and direction can be computed. Alternatively the horizontal wind can be described in terms of two components in a coordinate system which could be aligned with North as well. In this case the statistics of the mean wind vector are computed in the reference coordinate system; the magnitude of the fluctuations is described by a symmetric covariance matrix consisting of diagonal elements which are the variance of each component over the sample time period, and an off-diagonal element representing the covariance between the two fluctuating components. It is understood that any symmetric matrix can be diagonalized by the appropriate rotation, and in the case of the covariance matrix corresponding to the wind fluctuations this diagonalization has an important physical meaning.

The axes in which the covariance is null are called the principal axes. All the variance in this coordinate system is along the major or minor axis. Analyses (e.g. Beardsley et al., 1987) show that the

principal axes are usually closely aligned with topography in a coastal environment, and thus represent a natural coordinate system in which to work, as compared to a system aligned with the cardinal directions. The total variance along the major and minor axes is the same as the variance in the original coordinate system, and the ratio of the standard deviation along each axis to the mean speed is a measure of the amplitude of fluctuating winds. This description is adopted here even though it is not the most common description found in the meteorological literature, principally because it avoids difficulties associated with computing a direction associated with fluctuating wind speeds, because it determines the degree of polarization of wind fluctuations (the ratio of major to minor axis amplitudes) and because it is the description commonly adopted in the oceanographic literature. It should be emphasized that both descriptions are equally valid and give corresponding information: indeed the mean properties of the vector are identical in both descriptions, and a large standard deviation in wind speed would correspond to a large standard deviation along the principal axes.

Low-pass zero mean wind, temperature and pressure time series for selected stations are presented in Figure 2 to illustrate time coverage as well as synoptic and seasonal data variability. Each of the selected series is representative of the conditions observed in different regions of the Gulf, namely West Florida shelf, northeast coast, northwest coast, inner Gulf, southwest coast, Yucatán region. Short time data gaps in the series were filled out by interpolation using a second order polynomial fit with neighboring stations.

### 3. Average Climatology: The Mean

Time averaged values of the various properties observed at each station, based on the three year period 1 August 1990 - 31 July 1993 are illustrated in Figure 3 and summarized in Tables 2 through 5.

Mean wind vectors computed for each station are illustrated in Figure 3a along with contours of averaged atmospheric pressure. The mean wind vectors are generally westward, in the sense of the Trade winds. Mean wind speeds range between  $0.1 \text{ m s}^{-1}$  and  $4.4 \text{ m s}^{-1}$ . The largest averaged winds occur near the Yucatán peninsula where the direction of the mean is towards the southwest. In the central Gulf, the mean wind is directed towards the west, with speeds about  $3 \text{ m s}^{-1}$ . The smallest mean winds are found off the coast of west Florida, Alabama and Mississippi, with speeds ranging from  $0.1 \text{ m s}^{-1}$  to  $1.5 \text{ m s}^{-1}$ . Mean winds observed at the two southwest Gulf stations stand in contrast to other stations: the direction is southeastward and amplitudes are about  $2 \text{ m s}^{-1}$ . The direction is consistent with that of the Sierra Madre Oriental mountain range which appears to steer the winds towards the Isthmus of Tehuantepec. This mountain range is characterized by heights of 2000 m to 3000 m. Pico de Orizaba mountain which is within 100 km of the coast, exceeds 5600 m, and is among the tallest mountains of the North American continent. It is difficult to reconcile the mean wind directions provided by the RTW analysis with this extreme relief. Near Tehuantepec, the relief drops to a minimum elevation of 250 m at the 40 km wide Chivelas Pass. The results of the analysis presented here, consistent with the analysis of ship observations presented by Elliott [1979], suggest that the mountain range has a profound influence on the mean wind properties.

The time averaged atmospheric pressure generally increases from the southwest towards the northeast, with a uniform gradient, with the exception of the region surrounding the Yucatán peninsula. Standard

deviations of this variable are similar at all locations during the observation period, averaging about  $4 \times 10^2$  Pa, with slightly higher values at the westernmost stations.

Fluctuations in the wind over the three year period are represented as principal axes ellipses in Figure 3b. The direction of the major axis is almost perpendicular to the mean wind direction, and the magnitude of the fluctuations frequently exceeds that of the mean. The ratio of the minor to the major axis vary from 0.53 to 0.95 (Table 2), with higher values in the northeastern Gulf and lower values over the western Gulf, where a large fraction of the variability can be attributed to frontal incursions.

Time averaged wind stresses for each station are summarized in Table 3, they range from minimum values which are not significantly different from zero in the northeastern corner to maximum values exceeding  $4 \times 10^{-2}$  Pa around the Yucatán peninsula. These averaged wind stresses were interpolated to a 15' square latitude-longitude grid to produce the map illustrated in Figure 3c. These gridded values were in turn used to estimate the wind stress curl, mapped in Figure 3d. On the average the wind stress curl is positive over the west and southwest Gulf, and negative over the remaining portion. This pattern is consistent with the results of Elliott [1979], and contrast markedly with the wind stress curl computed by RTW, and used by Sturges [1993].

Time averaged air temperature and sea temperature are contoured in Figure 4e. Mean air temperatures range from 20.5 °C to 26.8 °C, increasing uniformly from the northwest towards the southeast. The average sea temperature ranges between 22.4 °C and 28 °C, increasing in the same direction. The standard deviations in air and water temperatures (Table 4) range around 6 °C throughout the Gulf. Water temperatures exceed air temperatures over the entire Gulf.

Although sensible heat exchange is expected to account for only a small amount of the available heat transfer between the atmosphere and the Gulf waters, the higher water temperature suggests that the heat due to conduction is transferred from the water to the atmosphere. Sensible heat, estimated according to

the formula suggested by Gill [1982], and using the variables presented in this study are mapped in Figure 3f. Values range between  $3.5 \text{ W m}^{-2}$  over the southern Gulf and  $22 \text{ W m}^{-2}$  over the north. These values represent between 10 and 30 % of the  $50 \text{ W m}^{-2}$  estimated by Budyko [1963] for the latent heat flux in the region.

#### 4. The Annual Cycle and Seasons

Seasonal amplitudes and phases are computed for each variable at each station by a least squares fit to a cosine with annual and semi-annual harmonics. The phase is determined relative to 0000Z 1 August 1990. Results of these analyses are summarized in Tables 6 and 7, and those of the annual harmonic are plotted in Figure 4.

The amplitude of the annual cycle of the zonal wind decreases in magnitude from the West Gulf, where it reaches 1 to  $1.2 \text{ m s}^{-1}$ , towards the central Gulf region where it has minimum values of  $0.4 \text{ m s}^{-1}$  (Figure 4a). Annual and semi-annual cycle amplitudes are up to 50 % smaller than the mean wind speeds in the eastern and northern Gulf and up to 90 % smaller in the south. Annual phases imply a maximum of the cycle during the winter season while semi-annual phases indicate a maximum during winter and late summer. The phase change between the southwestern Gulf and the central Gulf amounts to nearly four months, although the amplitude of the zonal component in the southwestern section is quite weak.

The annual cycle of the meridional wind decreases in amplitude from about  $2 \text{ m s}^{-1}$  in the northwestern Gulf coast to about  $0.5 \text{ m s}^{-1}$  in the south (Figure 4b). In the northern Gulf this amplitude compares in magnitude to the mean wind speed but in the southern region the mean wind speed is 10 times the annual cycle amplitude. Phases are negative and almost constant (around -45 days) throughout the Gulf, indicating maximum northward speeds during mid June and maximum southward speeds during mid December. Semi-annual amplitudes have a zonally varying pattern, with values around  $0.2 \text{ m s}^{-1}$  in both the East and West increasing to  $0.5 \text{ m s}^{-1}$  in the central region of the Gulf.

The amplitudes of the annual cycle of the atmospheric pressure range from  $0.82 \times 10^2$  to  $3.20 \times 10^2 \text{ Pa}$  (Figure 4c), about half of the total standard deviation at each station. Minimum amplitudes occur in the southeast and increase smoothly towards the northwest. The phase of the annual cycle progresses

westward with maximum values occurring during December and January. Semi-annual amplitudes are half the annual amplitude in most sites and have little spatial variation; the phase shows maximum values during December and late July.

Atmospheric and water temperature seasonal variabilities are very similar (Figures 4d,e). Annual cycle amplitudes increase from 1 °C to 8 °C, following the same spatial northward gradient pattern as the mean temperatures. Phase progresses in both cases from South to North, with a stronger gradient for atmospheric temperature and with water temperature lagging by 5-15 days. Maximum atmospheric (water) temperatures occur during mid July (early August) in the South and in late July to early August (mid August) in the North. Semi-annual to annual amplitude ratio ranges from approximately 0.04 in the North to 0.25 in the South. Phase advances northward from mid July in the South to mid August in the North for both temperatures.

Time series of atmospheric properties measured around the Gulf, as illustrated in Figure 2, and other statistics presented suggest that the weather in the Gulf can be roughly partitioned in two seasons: an extended winter when frontal incursions and cold air outbreaks are mainly responsible for the synoptic variability and a summer season, when the variability is relatively small except when tropical storms or even hurricanes have a profound effect on the climate. While statistics of the wind field differ little between spring and summer, SST patterns are similar between summer and fall. These differences suggest the most complete description is in terms of the four classical seasons, even though the variable analyzed vary for the most part between two states. Previous authors [Elliott, 1979; RTW] have also preferred to partition the variability in four seasons, and the corresponding discussion of the present results is also cast in terms of four equivalent seasons in order to facilitate comparison between the different studies.

An attempt was made to place the period of observations in a climatological perspective. The NDBC buoys which are located in the center of the Gulf have reported atmospheric pressure and temperature since 1977. Air temperature anomaly time series were formed by computing seasonal averages of the temperature at each site, and subtracting these from the original time series. Inspection of the resulting anomaly series clearly shows the effect of the strong El Niño event in 1983. In contrast, no significant anomaly is present during the period of observations. Maps of the  $700 \times 10^2$  Pa height anomalies prepared by the National Meteorology Center were reviewed, and no significant anomaly was detected over the Gulf of Mexico over the period. While the possible influence of interannual variability on the results presented here cannot be discounted entirely, the period August 1990 - August 1993 appears to have been reasonably representative of long term conditions over the Gulf of Mexico, at least by the two measures considered here.

Maps of seasonally averaged properties for spring (March, April and May) are illustrated in Figure 5. North of 24 °N, winds are directed towards the northwest, and near the Yucatán peninsula, winds are directed towards the southeast. The seasonally averaged atmospheric pressure mapped in Figure 5a increases from southwest to northeast, with a total difference of about  $5 \times 10^2$  Pa. The wind fluctuations (Figure 5b) are along principal axes which correspond closely to those computed for the three year average (Figure 3b): the major axis is nearly normal to the seasonally averaged wind speed, and exceeds the mean wind by a factor between two and three. The ellipticity of the variance ellipses ranges from 0.5 in the western Gulf to near unity in the east. Wind stress patterns (Figure 5c) are similar to the wind, and the corresponding curl (Figure 5d) is positive over the northwestern and southern Gulf and negative elsewhere. The direction of the wind stress is in close correspondence to the patterns described by Elliott [1979], but the amplitudes based on the observations presented here are two to three times larger. Accordingly the wind stress curl patterns correspond to those computed by Elliott for the same season, but

the amplitude of the curl is larger based on the current observations. Air and sea temperature increase from north to south, from about 22 °C to 26 °C, and the sensible heat flux increases from south to north, from a value near zero to heat fluxes exceeding 15 W m<sup>-2</sup> near the West Florida coast.

Summer conditions (Figure 6) differ from the spring in that the wind is more towards the north in the northern Gulf, and weaker than in the spring in the southern Gulf. The atmospheric pressure is about 100 Pa larger than in spring. Wind fluctuations (Figure 6c) are weaker than in spring. The ellipticity is closer to unity everywhere. The latter two results can be explained in terms of the near absence of frontal incursions during the summer. The region of negative wind stress curl extends towards the southwest, but without reaching the coast, although the wind stress curl is close to zero along the northern coast of Yucatán. Again the pattern of wind stress curl matches that presented by Elliott [1979], although with somewhat larger amplitudes. The air temperature is practically constant over the entire Gulf, and the sea temperature varies by only 2 °C. The small difference between air and sea temperatures result in insignificant latent heat fluxes between the ocean and the atmosphere.

There is a marked contrast between the summer and fall as frontal incursions begin to take effect. The direction of seasonally averaged wind is due west north of 24 °N (Figure 7a), and the isobars are also more nearly meridional. The amplitude of the fluctuations (Figure 7b) is larger than in summer, although the ellipticity remains close to unity. The distribution of seasonally averaged wind stress (Figure 7c) is more nearly uniform with the same change in direction as noted for the wind. The direction of wind stress matches Elliott's results, but amplitudes are again larger. The region of negative wind stress curl decreases in extent (Figure 7d), and the positive curl values increase over summer values in along the southwest coast, with a westward shift of the location of the maximum. A uniform gradient in air temperature begins to appear, increasing from 21 °C near the coast of Texas to values near 27 °C near the coast of Yucatán.

Distinct pools of colder sea water appear near the coast of Texas and Louisiana-Mississippi as the cold air outbreaks begin the cooling cycle and the river runoff decreases its temperature.

Seasonally averaged wind stress vectors for the winter season (Figure 8a) and isobars are similar to the fall, but the fluctuations (Figure 8b) are nearly twice as large during the winter and the ellipticity is near 0.5 in the western portion of the Gulf, reflecting the strong polarization of winds induced by the cold air outbreaks. Patterns of wind stress curl are more complicated than in any other season, with areas of positive curl extending over the Gulf from the coast of Texas and Mississippi. The detail of these patterns is suspect given the small number of actual observation stations, but it is noteworthy that the different patterns are consistent with those derived from ship observations. Seasonal air and sea temperature gradients reach maximum values during this season, with temperatures remaining near 25 °C near Yucatán, while minimum air temperatures reach 13 °C near Texas and minimum water temperatures reach 17 °C.

As noted earlier, the seasonal change of atmospheric parameters can really be described in terms of two seasons: fall and winter when frontal incursions dominate the variability, and spring-summer when wave activity can build to tropical storm or even hurricane intensity.

## 5. Summary

Patterns of wind stress and wind stress curl over the Gulf of Mexico based on contemporary observations over the entire Gulf are such that the direction of momentum transfer is generally towards the west, with the exception of the southwestern portion, where winds and wind stress are directed towards the south, presumably steered by the mountain range which borders the Gulf in this area.

Seasonal patterns of wind stress and wind stress curl derived from the observations reported here are in close agreement with the maps published by Elliott [1979] based on historical surface marine observations gridded onto  $1^{\circ}$  squares, but the amplitude of the stress estimates are usually larger than suggested by Elliott. Both studies suggest that the wind stress curl is negative over the northeastern portion of the Gulf and positive over the southwestern portion, with a nodal line extending from the Yucatán peninsula towards the Mexico-US border. These results differ significantly from the wind stress and wind stress curl estimates developed by RTW based on pressure maps derived from a numerical model. The wind stress estimated by RTW are generally directed towards the west on the southwestern boundary of the Gulf, towards the high mountain range which extends along the coast. Corresponding wind stress curls are negative everywhere within the Gulf.

Using the wind stress curl estimates suggested by RTW, Sturges [1993] proposes that the annual cycle of the western boundary current in the Gulf is driven by the annual variation in the wind stress curl. The wind stress curl patterns may be substantially different, as suggested by the analysis presented here, and it may be useful to reconsider the question of the forcing of the western boundary current based on these results. While such a consideration is beyond the scope of this work, it is noted that a negative wind stress curl is present over a large portion of the Gulf in all maps.

Vázquez de la Cerdá [1993] suggests that the circulation in the Bay of Campeche, the southern portion of the Gulf, beneath 22 °N, consists of a semi-permanent cyclonic gyre, the existence of which would be difficult to understand if the wind stress curl were permanently negative over the entire Gulf. The existence of an area of positive wind stress curl is compatible with such a circulation, as suggested by Vázquez de la Cerdá.

## Acknowledgments

The work presented here evolved as a result of a collaborative effort between the Center for Coastal Studies at the Scripps Institution of Oceanography, Dirección de Oceanografía de la Secretaría de Marina and Instituto de Geofísica, UNAM. The field work carried out in Mexico was made possible through consistent and gracious support from the Mexican Navy who provided ship time to support this effort. The help of the officers, staff and enlisted men of the Mexican Navy is gratefully acknowledged. Admiral Lopez-Lira, who was responsible for the Mexican Naval Oceanographic Research at the inception of this program was tremendously supportive and helped overcome innumerable administrative impediments in the initial stages. Admiral Vázquez de la Cerda, who took over Admiral Lopez-Lira's responsibilities midway through the program, continued to provide special support and even participated in some of the field work. It is obvious that without the constant support and encouragement provided by these officers, the work reported here could not have been carried out. Questions raised by two reviewers were most helpful in improving this manuscript, in addition conversations with Dan Cayan helped us evaluate the possible influence of interannual variability on the observations presented here. The Office of Naval Research supported this work through grant N00014-90J-1127.

## References

Beardsley, R.C., C.E. Dorman, C.A. Friehe, L.K. Rosenfeld, and C.D. Winant, 1987: Local atmospheric forcing during the Coastal Ocean Dynamics Experiment, 1. A description of the marine boundary layer and atmospheric conditions over a northern California upwelling region. *Journal of Geophysical Research-Oceans*. (92)C2, 1467-1488.

Budyko, M.I., 1963: Atlas of heat balance of the Earth. Moscow: *Academy of Sciences*.

Elliott, B.A., 1979: Anticyclonic rings and the energetics of the circulation of the Gulf of Mexico. Ph. D. Thesis, *Texas A&M University*.

Gill, A.E., 1982: Atmosphere-Ocean Dynamics. *Academic Press*. New York. 663 pp .

Hamilton, G.D., 1980: NOAA Data Buoy Office programs. *Bull. A.M.S.*, (61) 9, 1012-1017.

Large, W.G., and S. Pond, 1981: Open ocean momentum flux measurements in moderate to strong winds. *Journal of Physical Oceanography*, (11) 3, 324-336.

Rhodes, R.C., J.D. Thompson, and A.J. Wallcraft, 1989: Buoy-calibrated winds over the Gulf of Mexico. *Journal of Atmospheric and Oceanic Technology*, (6) 4, 608-623.

Sturges, W., 1993: The annual cycle of the western boundary current in the Gulf of Mexico. *Journal of Geophysical Research-Oceans*, (98)C10, 18053-18068.

Vázquez de la Cerdá, A.M., 1993: Bay of Campeche cyclone. Ph.D. Thesis, *Texas A&M University*.

**Table 1: Meteorological Stations Positions and Coast Orientation.**

Name	Longitude	Latitude	Coast Orientation
	West	North	Degrees True North
<b>SVLS1</b>	79° 19.02'	31° 57.00'	150°
<b>SAUF1</b>	80° 44.10'	29° 51.42'	150°
<b>LKWF1</b>	79° 58.02'	26° 36.72'	150°
<b>SPGF1</b>	79° 00.00'	26° 41.52'	150°
<b>VENF1</b>	81° 33.00'	27° 04.20'	150°
<b>42003</b>	84° 05.16'	25° 56.16'	
<b>CSBF1</b>	84° 38.58'	29° 40.32'	90°
<b>42007</b>	87° 13.80'	30° 05.40'	90°
<b>MPCL1</b>	87° 24.18'	29° 24.18'	90°
<b>GDIL1</b>	88° 02.58'	29° 16.02'	90°
<b>BURL1</b>	88° 34.32'	28° 54.30'	90°
<b>42001</b>	88° 20.82'	25° 55.68'	
<b>42002</b>	92° 24.78'	25° 55.56'	
<b>GBCL1</b>	92° 52.02'	27° 48.00'	
<b>SRST2</b>	93° 57.00'	29° 40.20'	60°
<b>PTAT2</b>	96° 57.00'	27° 49.68'	60°
<b>Tuxpan</b>	97° 06.00'	21° 04.20'	150°
<b>Veracruz</b>	96° 03.60'	19° 12.00'	150°
<b>Coatzacoalcos</b>	94° 22.50'	18° 09.00'	115°
<b>Cayo Arcas</b>	91° 54.00'	20° 15.00'	
<b>Isla Peres</b>	89° 37.50'	22° 30.00'	
<b>Isla Mujeres</b>	86° 30.00'	21° 18.00'	80°

**Table 2: Wind Statistics**  
Time period: August 1990 to August 1993.

Name	Mean Wind				Principal Axis			Ratio Min/Maj
	Zonal $\text{m s}^{-1}$	Meridional $\text{m s}^{-1}$	Speed $\text{m s}^{-1}$	Direction Deg. True	Major $\text{m s}^{-1}$	Minor $\text{m s}^{-1}$	Direction Deg. True	
SVLS1	-0.47	-0.19	0.51	248	5.15	3.57	266	0.6935
SAUF1	-0.56	-0.42	0.70	233	3.73	3.10	182	0.8311
LKWF1	-2.51	1.02	2.71	292	3.83	3.64	105	0.9509
SPGF1	-1.83	0.41	1.88	283	3.16	2.21	97	0.6983
VENF1	-0.56	-0.75	0.94	217	3.09	2.57	122	0.8328
42003	-2.87	-0.17	2.87	267	4.06	3.59	149	0.8828
CSBF1	-0.01	-0.11	0.11	188	2.74	2.15	81	0.7830
42007	-1.12	-0.30	1.15	255	3.96	3.60	200	0.9092
MPCL1	-1.33	0.13	1.34	276	4.43	3.76	112	0.8504
GDIL1	-1.29	-0.44	1.36	251	3.75	3.43	182	0.9142
BURL1	-1.49	-0.35	1.53	257	4.74	4.01	172	0.8458
42001	-3.06	-0.08	3.06	268	4.20	3.03	167	0.7220
42002	-3.27	0.77	3.36	283	4.54	2.89	167	0.6369
GBCL1	-2.61	1.31	2.91	297	4.92	3.53	171	0.7174
SRST2	-1.25	1.34	1.84	317	3.96	2.91	170	0.7363
PTAT2	-2.88	0.38	2.91	278	4.80	2.56	158	0.5330
Tuxpan	-1.65	0.26	1.67	279	3.51	2.40	276	0.6849
Veracruz	1.11	-1.83	2.14	149	4.01	2.85	119	0.7121
Coatzacoalcos	0.68	-2.37	2.46	164	2.65	2.49	219	0.9399
Cayo Arcas	-3.98	-1.93	4.43	244	4.27	2.82	144	0.6608
Isla Peres	-3.95	-1.55	4.24	249	4.18	2.98	148	0.7119
Isla Mujeres	-3.91	-0.96	4.03	256	3.52	2.64	186	0.7512

**Table 3: Wind Stress Statistics**  
Time period: August 1990 to August 1993.

Name	Zonal Component				Meridional Component				Mean Wind Stress	
	Mean	Min	Max	S.Dev.	Mean	Min	Max	S.Dev.	Magnitude	Direction
	10 <sup>-1</sup> Pa	10 <sup>-1</sup> Pa	10 <sup>-1</sup> Pa	10 <sup>-1</sup> Pa	10 <sup>-1</sup> Pa	Deg. True				
SVLS1	-0.0690	-4.1320	4.4340	0.5990	-0.0760	-4.9540	3.4050	0.6880	0.1026	222
SAUF1	-0.0697	-2.1324	1.3788	0.2893	-0.0689	-3.0404	2.5722	0.4168	0.0980	225
LKWF1	-0.2000	-3.3880	1.3390	0.3430	0.0790	-2.3070	3.3400	0.2930	0.2150	292
SPGF1	-0.1539	-2.2519	1.1643	0.3294	0.0018	-1.0902	1.0295	0.1859	0.1539	271
VENF1	-0.0105	-1.3244	1.6994	0.2484	-0.0542	-1.8846	1.1632	0.2486	0.0552	191
42003	-0.2840	-3.5510	2.2240	0.4810	-0.0216	-2.9282	2.5116	0.4768	0.2848	266
CSBF1	0.0215	-0.6969	1.1761	0.1983	0.0025	-0.8921	0.8769	0.1385	0.0216	83
42007	-0.1120	-3.2930	2.1180	0.4150	-0.0599	-3.1329	2.6939	0.4564	0.1270	242
MPCL1	-0.1440	-4.6420	3.0380	0.5130	-0.0157	-3.1534	2.5096	0.4123	0.1449	264
GDIL1	-0.1163	-3.2574	1.7065	0.3571	-0.0810	-3.5540	2.2140	0.4190	0.1417	235
BURL1	-0.1670	-5.4880	2.8170	0.5250	-0.0620	-5.5520	5.0710	0.6550	0.1781	250
42001	-0.2879	-3.0824	1.4255	0.3889	-0.0215	-3.1730	3.1378	0.5106	0.2887	266
42002	-0.3240	-3.2880	1.0960	0.3880	0.0600	-3.2210	3.3880	0.5710	0.3295	280
GBCL1	-0.2590	-4.2500	2.3890	0.4310	0.1260	-4.8830	5.3280	0.6160	0.2880	296
SRST2	-0.1128	-2.1161	1.7378	0.2961	0.1376	-1.6189	2.8314	0.4085	0.1779	321
PTAT2	-0.2704	-2.6095	1.0194	0.3497	0.0340	-3.1030	3.5660	0.5560	0.2725	277
Tuxpan	-0.1441	-3.0549	1.2264	0.3728	0.0070	-1.8357	1.7437	0.2135	0.1443	273
Veracruz	0.1560	-2.0470	3.7720	0.5170	-0.1970	-3.4640	1.8010	0.4300	0.2513	142
Coatzacoalcos	0.0546	-1.4080	1.9848	0.2125	-0.1878	-1.7946	0.8736	0.2467	0.1956	164
Cayo Arcas	-0.4280	-3.5580	1.3940	0.4660	-0.1990	-3.3770	1.8600	0.4990	0.4720	245
Isla Peres	-0.3950	-3.2860	1.3680	0.4160	-0.1676	-3.1386	2.0871	0.4476	0.4291	247
Isla Mujeres	-0.3445	-2.5342	0.5546	0.3053	-0.0431	-2.8063	1.7179	0.3687	0.3472	263

**Table 4: Pressure and Temperature Statistics**

Time period: August 1990 to August 1993.

Name	Air Pressure				Air Temperature				Water Temperature			
	Mean $10^2$ Pa	Min $10^2$ Pa	Max $10^2$ Pa	S.Dev. $10^2$ Pa	Mean °C	Min °C	Max °C	S.Dev. °C	Mean °C	Min °C	Max °C	S.Dev. °C
SVLS1	1018.2	1001.5	1035.1	5.10	18.72	-0.20	30.80	6.27	15.47	10.10	24.00	3.65
SAUF1	1017.9	1003.6	1031.9	4.30	20.51	3.20	33.90	5.70	22.49	11.20	30.80	5.04
LKWF1	1017.7	1006.4	1028.2	3.30	25.29	14.90	32.30	2.90	26.96	19.80	30.80	2.41
SPGF1	1017.5	1006.3	1028.4	3.40	24.68	15.10	31.10	3.12	26.78	20.50	32.30	2.38
VENF1	1017.5	1005.9	1029.1	3.50	21.90	7.40	33.59	4.72	24.05	14.39	32.79	4.68
42003	1017.1	1006.2	1028.1	3.40	24.99	15.60	32.00	3.08	26.96	21.20	32.79	1.97
CSBF1	1017.8	1004.0	1031.7	4.30	20.59	1.90	31.90	6.21				
42007	1017.4	1003.7	1032.0	4.40	21.56	2.90	32.60	6.22	22.73	10.39	32.90	5.72
MPCL1	1017.4	1003.4	1031.8	4.30	21.78	5.30	34.20	5.52	23.68	14.39	33.20	4.32
GDIL1	1017.3	1003.5	1032.1	4.40	21.02	2.50	33.29	6.17	23.00	6.69	34.00	6.12
BURL1	1017.3	1003.3	1031.0	4.30	21.06	2.70	33.00	6.23				
42001	1016.6	1004.7	1028.5	3.60	24.26	13.70	32.00	3.52	25.63	20.10	33.50	3.07
42002	1016.0	1002.5	1029.4	4.10	24.48	13.90	32.20	3.55	25.63	19.88	33.09	2.95
GBCL1	1016.7	1002.7	1030.8	4.30	22.96	9.20	31.20	4.55	25.47	19.30	31.80	3.39
SRST2	1017.1	1001.7	1033.6	5.00	20.47	-0.20	33.90	6.79				
PTAT2	1015.6	999.2	1032.5	5.00	21.24	3.30	30.30	5.90	22.38	8.90	32.20	5.68
Tuxpan	1013.7	988.8	1040.9	6.60	24.36	12.06	34.81	4.07	25.82	16.55	29.93	2.62
Veracruz	1013.1	999.2	1030.2	4.10	24.53	15.30	33.75	3.07	27.96	24.05	29.95	1.33
Coatzacoalcos	1012.8	998.1	1027.7	3.60	25.59	16.79	34.43	2.94	26.89	21.62	31.34	1.91
Areas	1013.6	1000.0	1026.8	3.80	26.79	18.26	35.15	2.84	26.89	22.49	29.98	1.76
Isla Peres	1014.3	993.5	1035.8	4.60	25.64	16.18	34.90	3.16	26.72	20.40	31.19	2.49
Isla Mujeres	1014.7	992.2	1036.7	4.40	26.52	21.04	31.97	1.80	26.99	17.42	29.69	1.32

**Table 5: Sensible Heat Upward Flux Statistics**

Time period: August 1990 to August 1993.

Name	Mean W m <sup>-2</sup>	Min W m <sup>-2</sup>	Max W m <sup>-2</sup>	S.Dev. W m <sup>-2</sup>
SVLS1	-5.67	-284.10	273.65	40.46
SAUF1	8.06	-161.47	171.78	21.69
LKWF1	7.93	-101.70	124.01	10.09
SPGF1	12.23	-18.79	103.91	12.20
VENF1	11.27	-81.45	129.47	17.64
42003	17.64	-31.59	170.40	24.01
CSBF1				
42007	13.02	-89.20	280.03	28.51
MPCL1	16.32	-175.93	261.17	28.70
GDIL1	15.56	-61.50	254.69	26.33
BURL1				
42001	12.02	-35.28	164.55	19.84
42002	10.41	-28.12	168.05	20.31
GBCL1	19.53	-58.32	289.43	30.29
SRST2				
PTAT2	11.41	-151.25	242.12	25.09
Tuxpan	11.77	-73.15	232.13	27.83
Veracruz	21.89	-72.16	244.60	31.57
Coatzacoalcos	5.73	-88.64	141.03	17.78
Cayo Arcas	3.52	-64.07	103.43	18.37
Isla Peres	5.24	-59.46	101.61	18.14
Isla Mujeres	7.11	-70.80	93.90	12.18

**Table 6: Wind Seasonal Cycles**

Time period: August 1990 to August 1993. Phase origin time is 00Z August 1 1990.

Name	Annual Cycle				Semi-Annual Cycle			
	Zonal Wind		Meridional Wind		Zonal Wind		Meridional Wind	
	Amplitude m s <sup>-1</sup>	Phase Days						
SVLS1	0.56	-133	2.21	-48	0.94	-7	0.44	10
SAUF1	0.89	-163	1.80	-45	0.93	-12	0.17	5
LKWF1	0.50	-143	1.10	-67	0.86	0	0.22	-11
SPGF1	0.91	-249	0.70	-40	0.96	7	0.17	-25
VENF1	0.87	-241	0.66	-59	0.23	6	0.32	-4
42003	0.59	-228	1.07	-65	0.92	14	0.26	-19
CSBF1	1.02	-224	1.12	-50	0.54	-8	0.20	-17
42007	0.91	-225	1.75	-50	0.90	-1	0.24	42
MPCL1	0.75	-227	1.44	-53	1.05	-3	0.23	-45
GDIL1	0.65	-219	1.91	-51	0.80	-1	0.20	-44
BURL1	0.78	-230	2.00	-50	1.12	-2	0.30	-33
42001	0.17	-271	1.61	-51	0.86	19	0.39	-31
42002	0.20	-266	1.46	-49	0.65	12	0.44	-32
GBCL1	0.31	-206	1.79	-48	0.58	4	0.49	40
SRST2	0.55	-193	2.32	-42	0.80	-3	0.33	20
PTAT2	1.44	-215	2.66	-26	0.57	-10	0.02	-34
Tuxpan	0.62	-92	0.42	-55	0.62	40	0.13	8
Veracruz	1.28	-234	0.77	-67	0.18	21	0.31	-12
Coatzacoalcos	0.92	-206	0.26	55	0.10	-18	0.25	-5
Cayo Arcas	0.50	-261	0.53	-78	0.61	-31	0.26	16
Isla Peres	0.71	-255	0.76	-54	0.37	25	0.65	27
Isla Mujeres	0.73	-183	1.01	-79	0.53	20	0.28	-6

**Table 7: Pressure and Temperature Seasonal Cycles**

Time period: August 1990 to August 1993. Phase origin time is 00Z August 1 1990.

	Atmospheric Pressure		Annual Cycle		Water Temperature		Atmospheric Pressure		Semi-Annual Cycle		Water Temperature		
	Atmospheric Pressure		Atmospheric Temperature		Water Temperature		Atmospheric Pressure		Atmospheric Temperature		Water Temperature		
	Name	Amplitude $10^2$ Pa	Phase Days	Amplitude $^{\circ}$ C	Phase Days	Amplitude $^{\circ}$ C	Phase Days	Amplitude $10^4$ Pa	Phase Days	Amplitude $^{\circ}$ C	Phase Days	Amplitude $^{\circ}$ C	Phase Days
SVLS1	2.32	-234		7.56	-1	6.79	4	1.10	-33	0.34	-17	2.78	5
SAUF1	1.81	-226		6.45	0	6.86	5	1.15	-26	0.44	-18	0.55	-13
LKWF1	0.87	-208		3.43	2	3.23	10	1.54	-18	0.16	-19	0.17	17
SPGF1	0.89	-205		3.58	7	3.12	11	1.58	-19	0.24	14	0.28	8
VENF1	1.53	-215		5.13	-1	6.38	-1	1.31	-19	0.08	6	0.35	25
42003	1.61	-231		3.50	4	2.39	8	1.38	-17	0.31	4	0.52	18
CSBF1	2.23	-226		7.36	-7			1.03	-28	0.32	16		
42007	2.45	-230		7.48	-7	7.64	0	0.99	-23	0.36	12	0.20	14
MPCL1	2.30	-232		6.25	-6	5.98	4	1.05	-23	0.13	20	0.28	-15
GDIL1	2.42	-232		7.46	-9	7.90	-5	1.04	-22	0.21	31	0.18	-31
BURL1	2.11	-231		7.66	-4			1.03	-19	0.13	-24		
42001	1.82	-233		4.20	3	4.18	16	1.34	-16	0.27	-20	0.34	-25
42002	2.14	-238		4.22	4	3.97	14	1.22	-12	0.28	-7	0.41	4
GBCL1	2.36	-238		5.30	-4	4.81	16	1.17	-15	0.27	0	0.61	-8
SRST2	3.20	-238		8.31	-11			1.03	-17	0.55	42		
PTAT2	3.01	-237		7.15	-8	7.44	-3	1.24	-10	0.92	-25	1.22	-25
Tuxpan	2.19	-246		3.93	-14			1.25	-7	0.99	-11	0.98	4
Veracruz	1.99	-238		2.82	-16	0.65	14	1.09	-7	0.88	-2	0.23	-9
Coatzacoalcos	1.90	-236		2.51	-22	1.78	8	1.18	-6	0.73	-8	0.86	8
Cayo Arcas	1.55	-237		2.58	-13	2.36	14	1.37	-7	0.24	-4	0.17	4
Isla Peres	1.36	-235		2.88	1	3.33	10	1.33	-9	0.15	-40	0.30	23
Isla Mujeres	0.82	-228		1.65	-3	1.50	5	1.35	-13	0.08	14	0.17	-24

## List of Figures

Figure 1 : Gulf of Mexico. Meteorological stations locations and Gulf bathymetry.

Figure 2: Observations Time Series. Zero mean low-pass filtered time series for selected locations in the Gulf of Mexico. Meridional and zonal wind ( $\text{m s}^{-1}$ ), atmospheric pressure (Pa), and atmospheric and water temperatures ( $^{\circ}\text{C}$ ).

Figure 3: Averaged Fields for August 1990 to August 1993. (a) Mean winds and atmospheric pressure, pressure contour units in  $10^2 \text{ Pa}$ , arrow sizes are proportional to wind magnitude in  $\text{m s}^{-1}$ ; (b) Wind principal axis, arrows represent the wind major axis magnitude and direction in  $\text{m s}^{-1}$ ; (c) Mean wind stress, arrow size proportional to wind stress magnitude in  $\text{Pa}$  ; (d) Mean wind stress curl, contours units in  $10^{-9} \text{ Pa cm}^{-1}$ ; (e) Mean air and sea temperatures in  $^{\circ}\text{C}$ , broken lines represent air temperatures and solid lines water temperatures in  $^{\circ}\text{C}$ ; (f) Mean sensible Heat Upward Flux Contours in  $\text{W m}^{-2}$ .

Figure 4: Annual Cycle Amplitudes and Phases. Phases in days with time origin at 0000Z August 1 1990. (a) zonal wind component, amplitude in  $\text{m s}^{-1}$ ; (b) meridional wind component, amplitude in  $\text{m s}^{-1}$ ; (c) atmospheric pressure, amplitude in  $10^2 \text{ Pa}$ ; (d) atmospheric temperature, amplitude in  $^{\circ}\text{C}$ ; (e) Sea surface temperature, amplitude in  $^{\circ}\text{C}$ .

Figure 5: Spring (March, April, May). (a) Averaged winds and atmospheric pressure, pressure contour units in  $10^2$  Pa, arrow sizes are proportional to wind magnitude in  $\text{m s}^{-1}$ ; (b) Wind principal axis, arrows represent the wind major axis magnitude and direction in  $\text{m s}^{-1}$ ; (c) Averaged wind stress, arrow size proportional to wind stress magnitude in Pa; (d) Averaged wind stress curl, contour units in  $10^{-9}$   $\text{Pa cm}^{-1}$ ; (e) Averaged air and sea temperatures in  $^{\circ}\text{C}$ , broken lines represent air temperatures and solid lines water temperatures in  $^{\circ}\text{C}$ ; (f) Averaged sensible heat upward flux contours in  $\text{W m}^{-2}$ .

Figure 6: Summer (June, July, August). As in Figure 5.

Figure 7: Fall (September, October, November). As in Figure 5.

Figure 8: Winter (December, January, February). As in Figure 5.

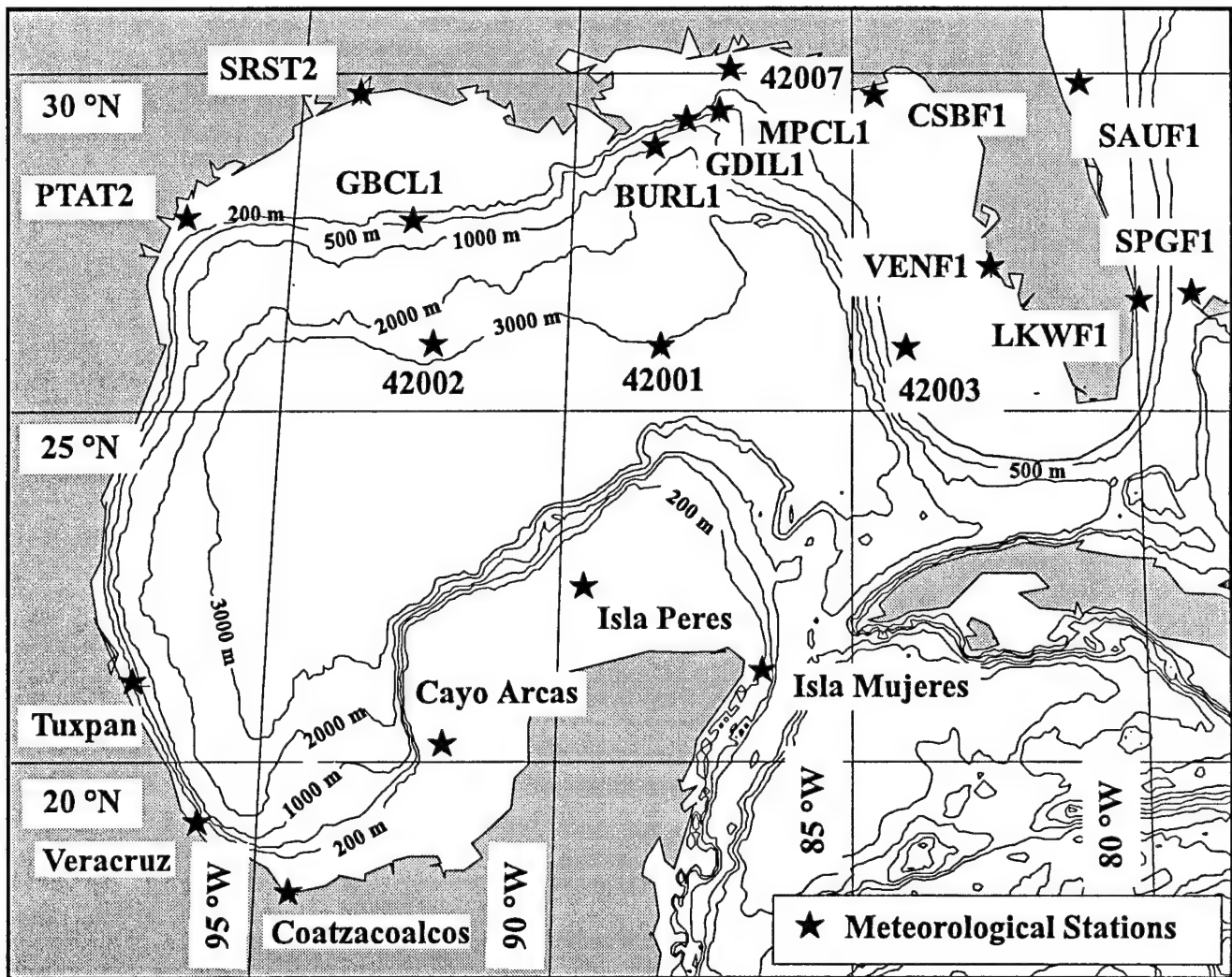


Fig 1

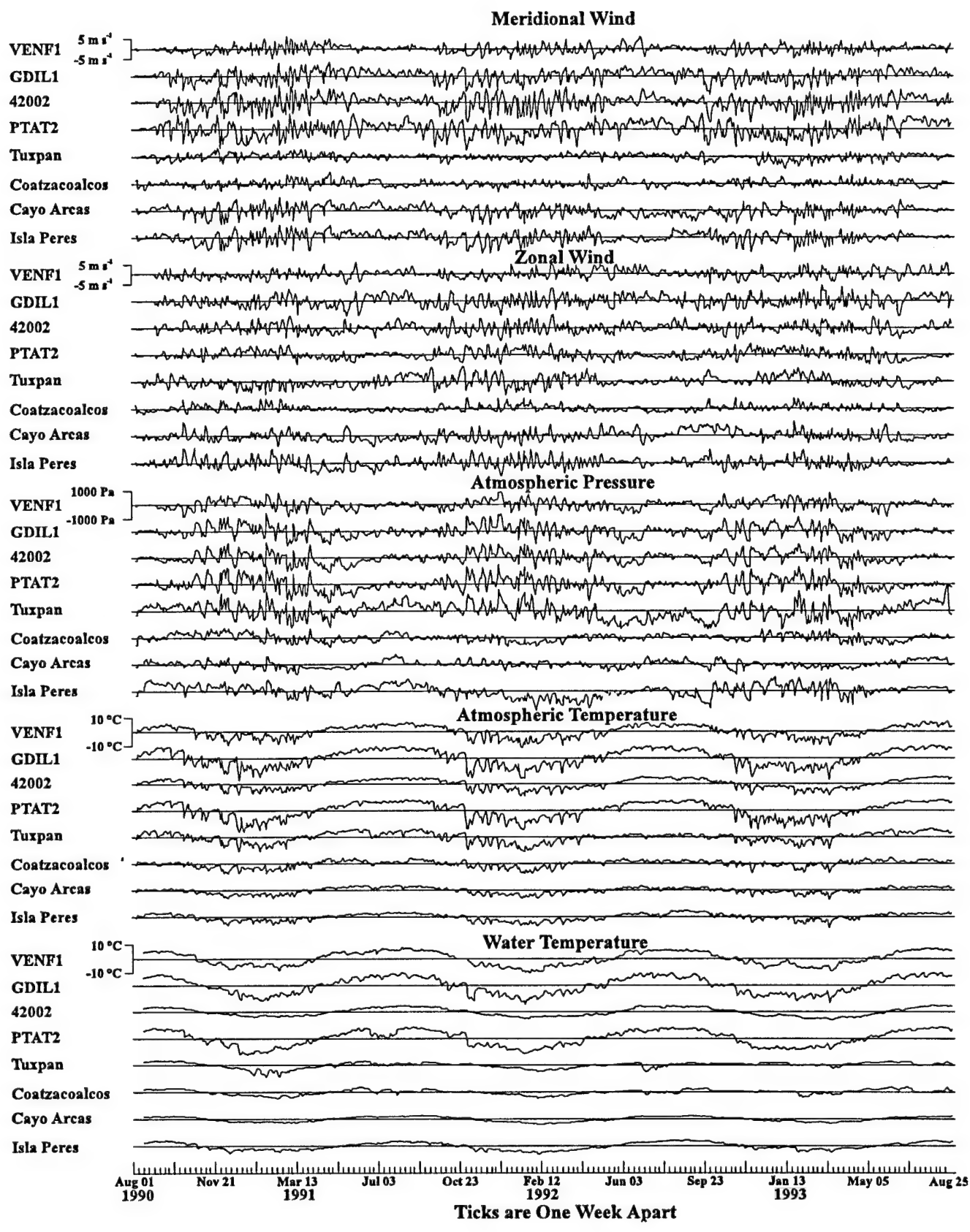


Fig. 2

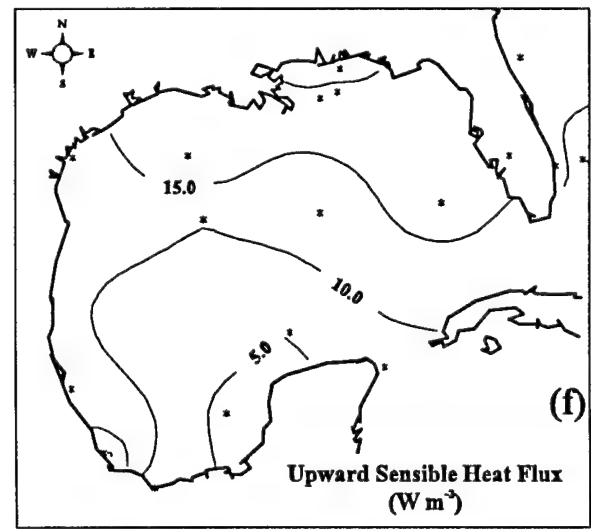
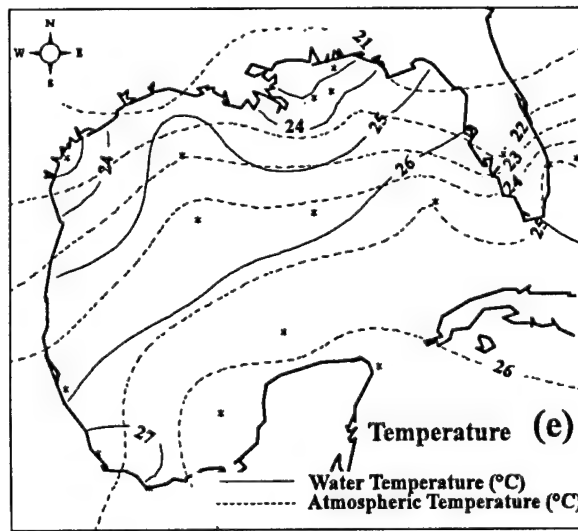
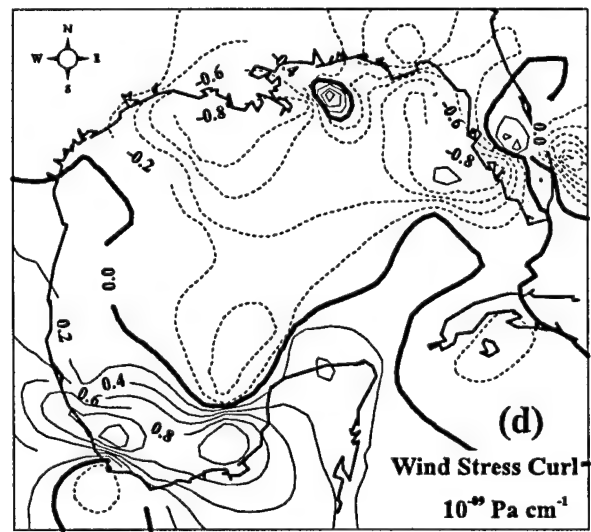
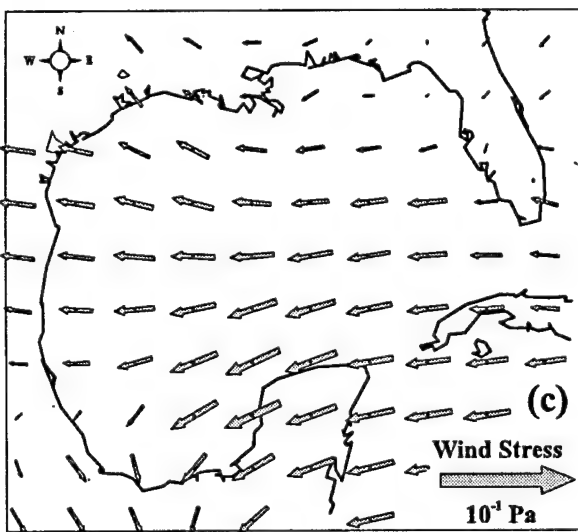
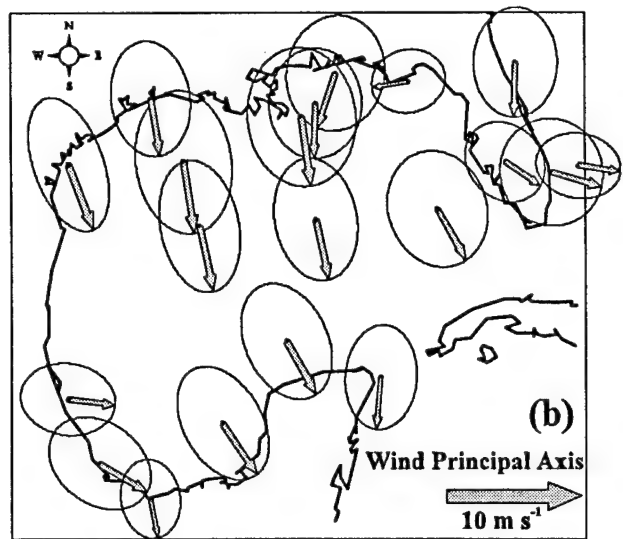
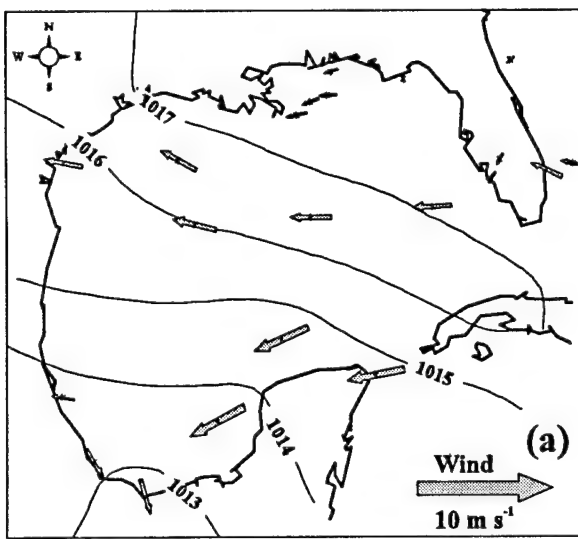


Fig 3

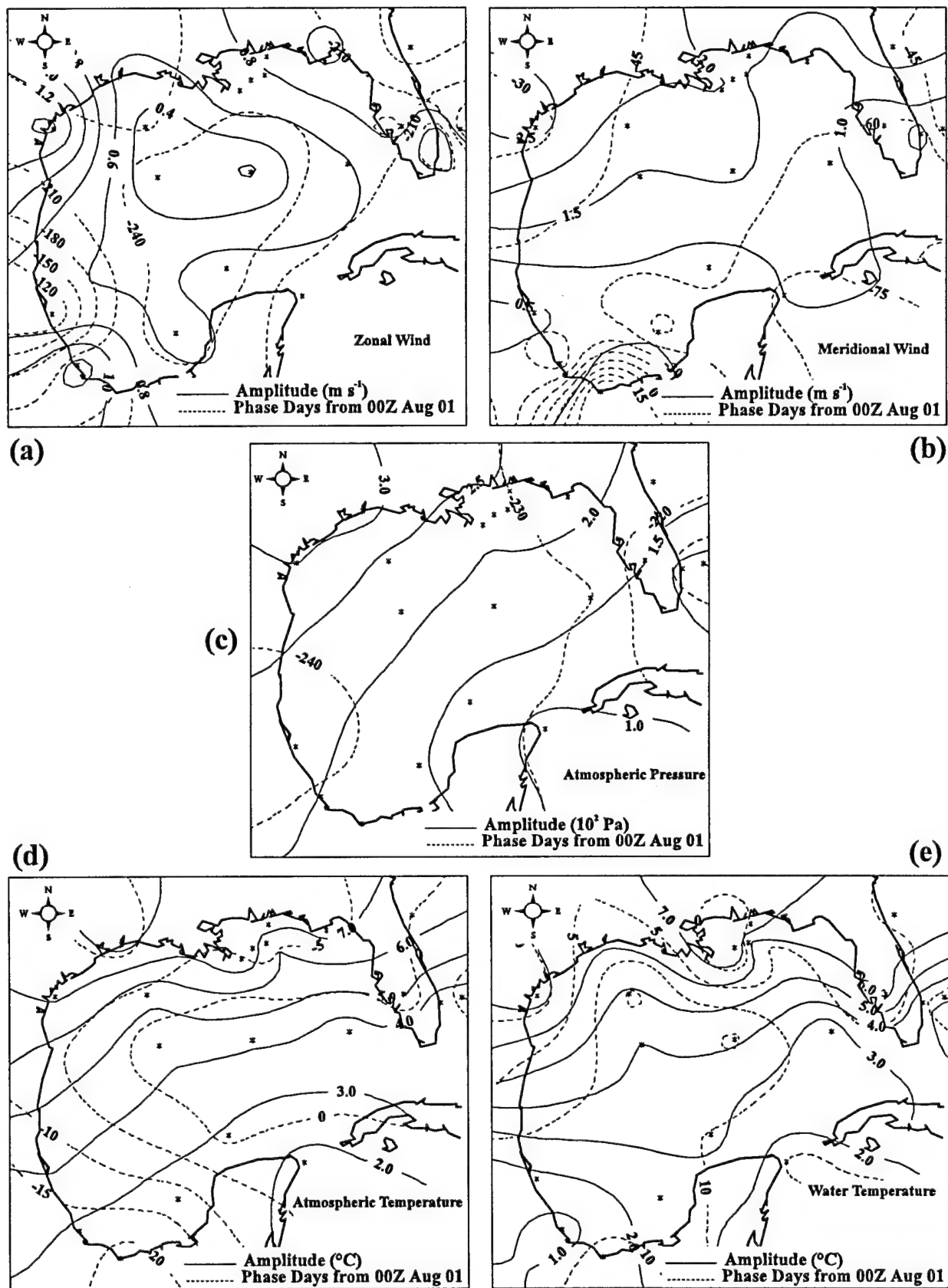


Fig 4

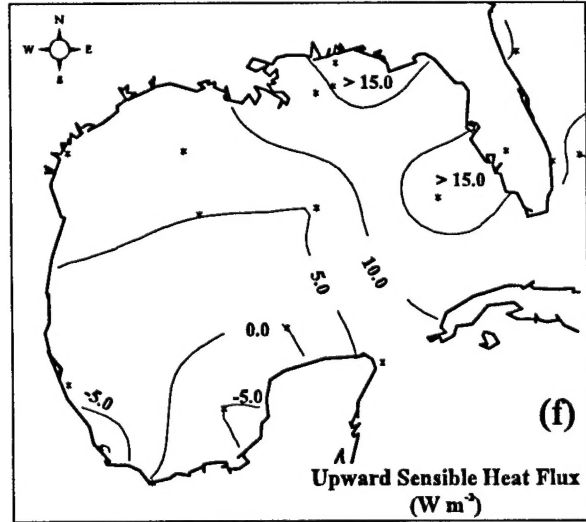
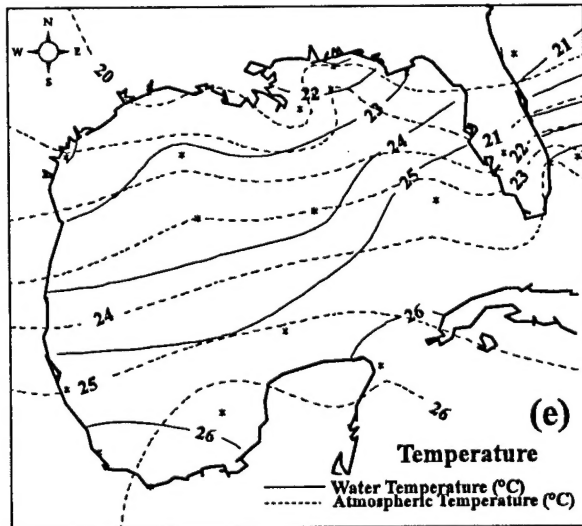
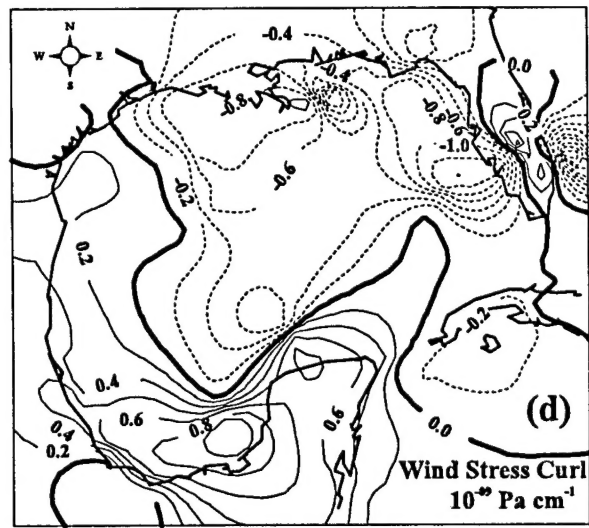
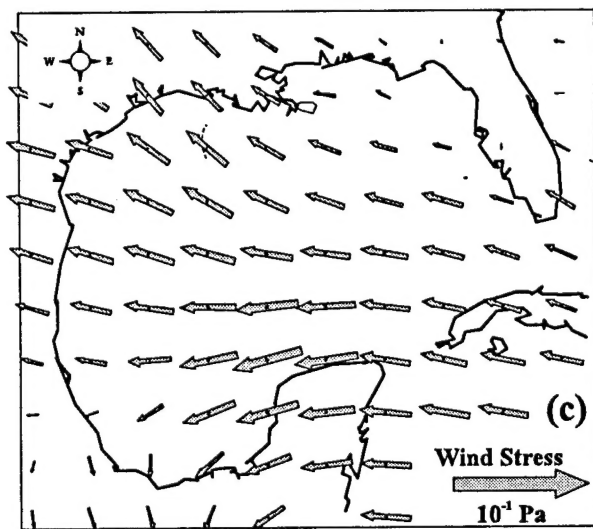
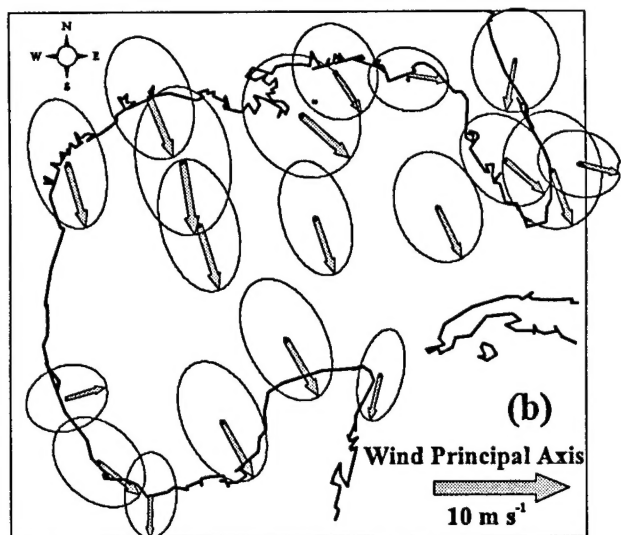
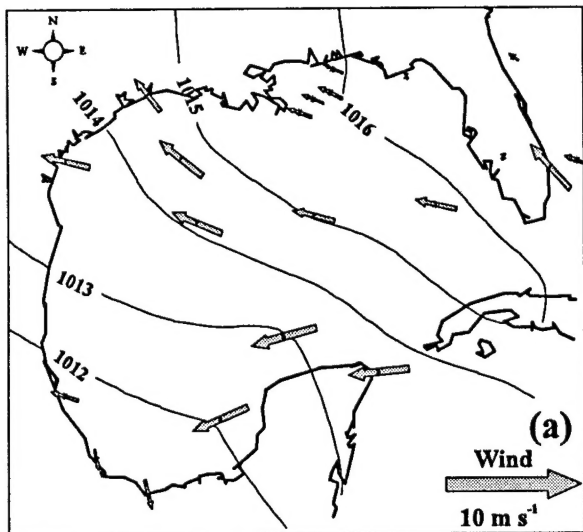


Fig 5

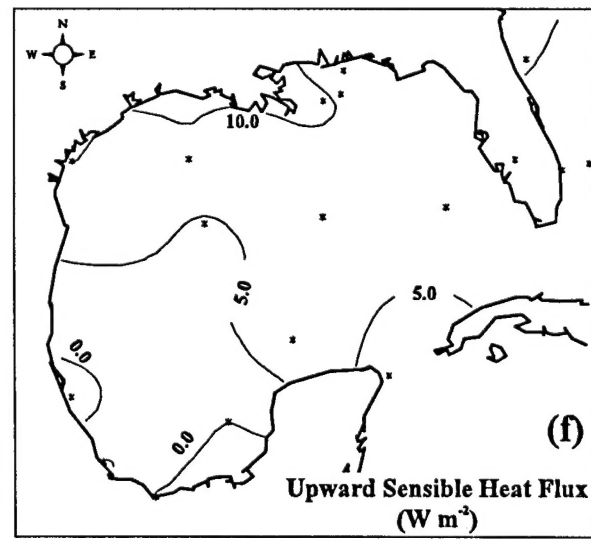
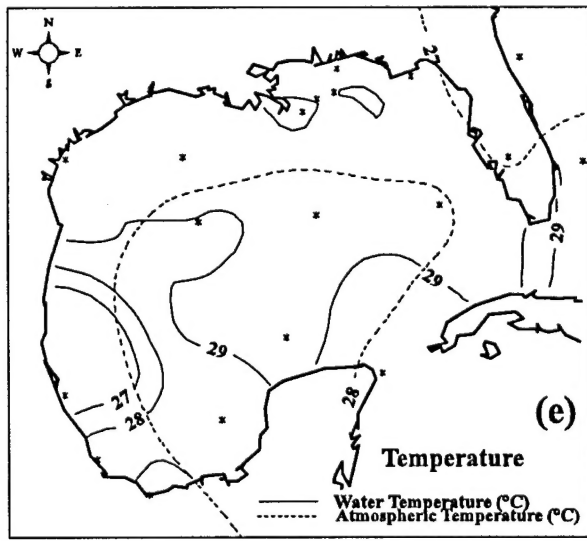
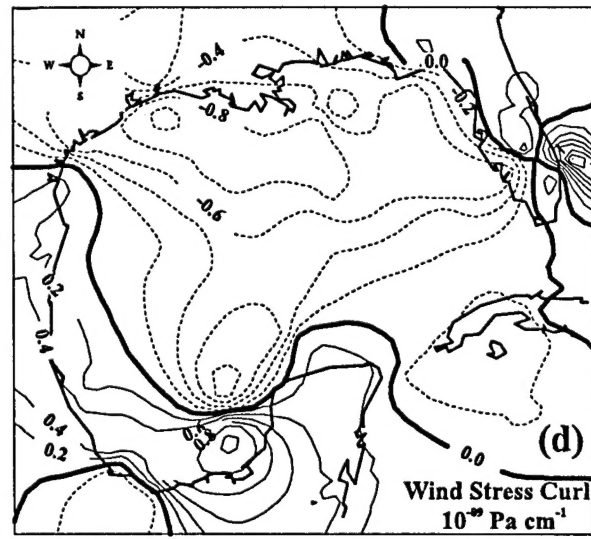
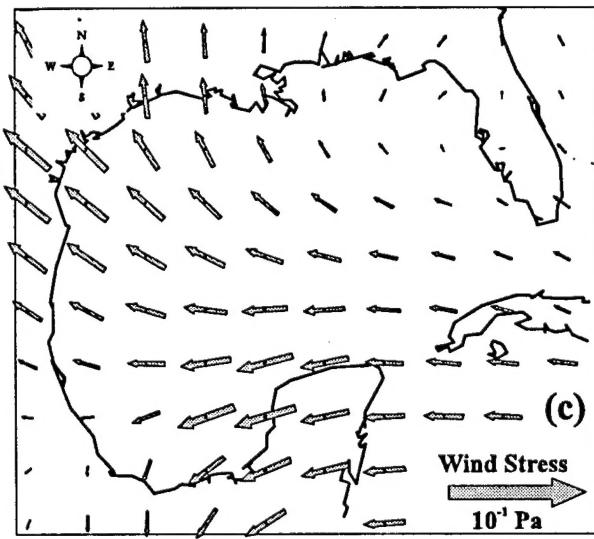
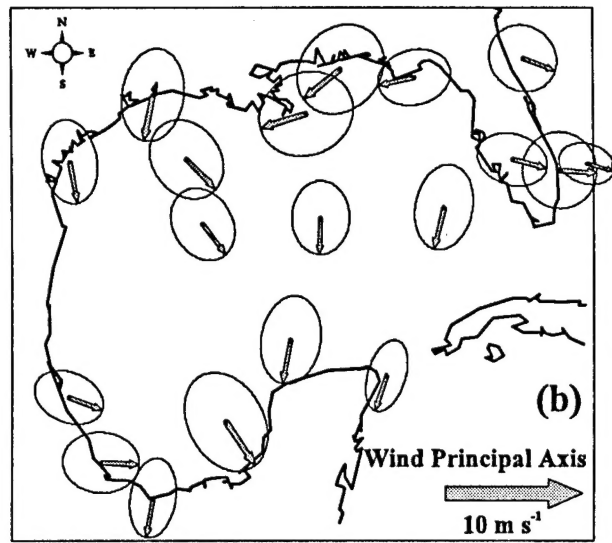
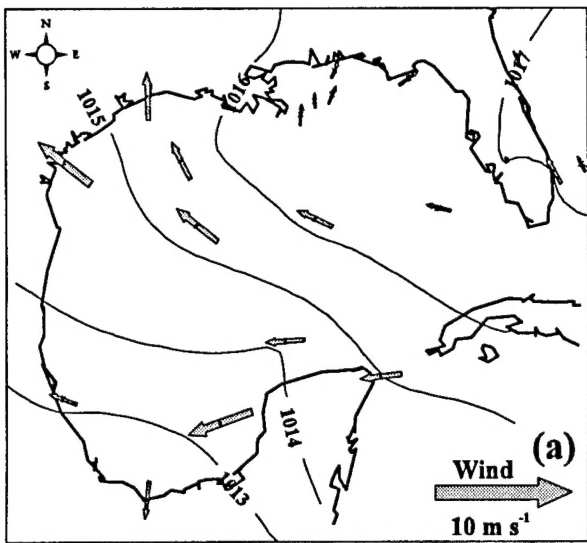


Fig 6

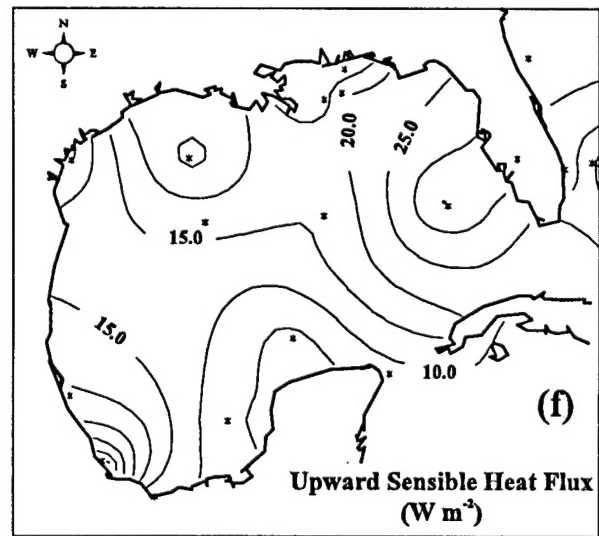
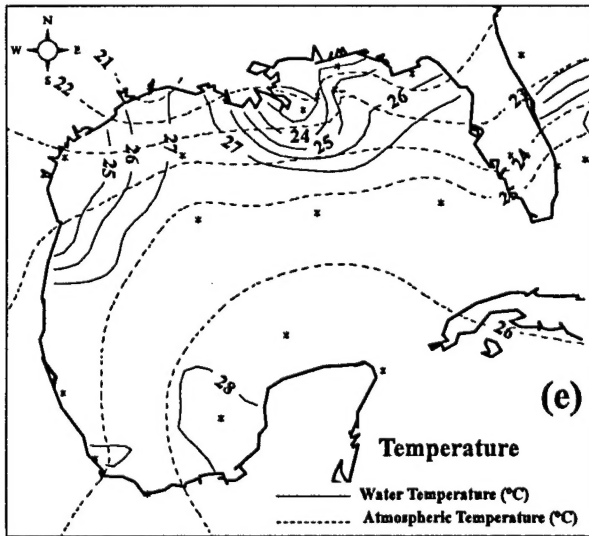
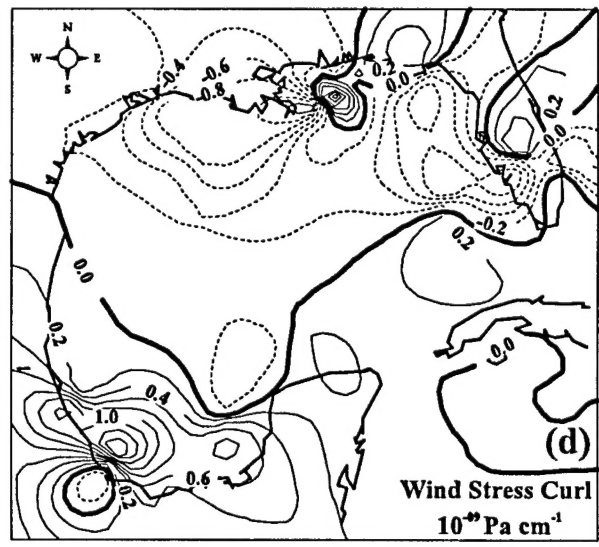
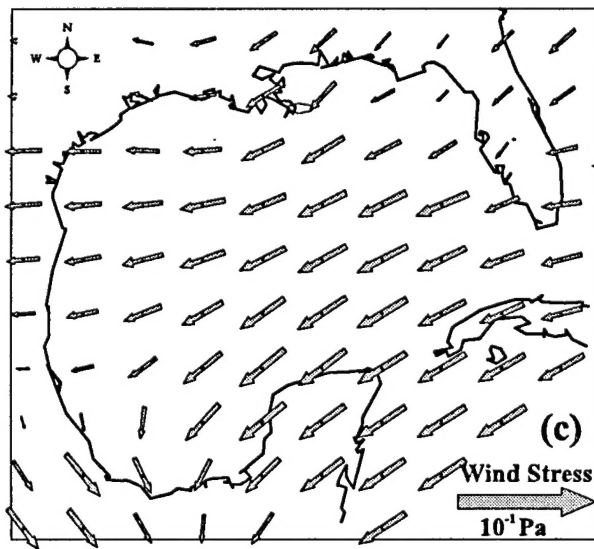
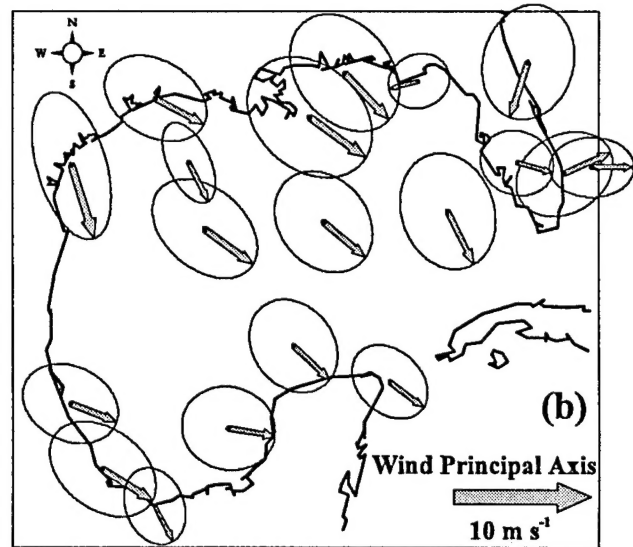
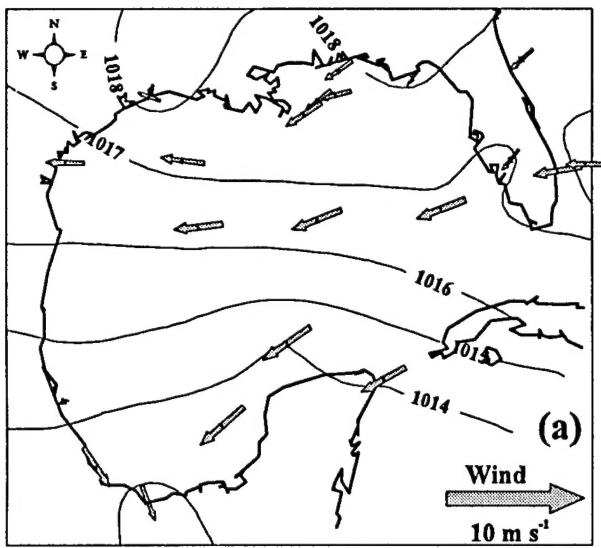


Fig 7

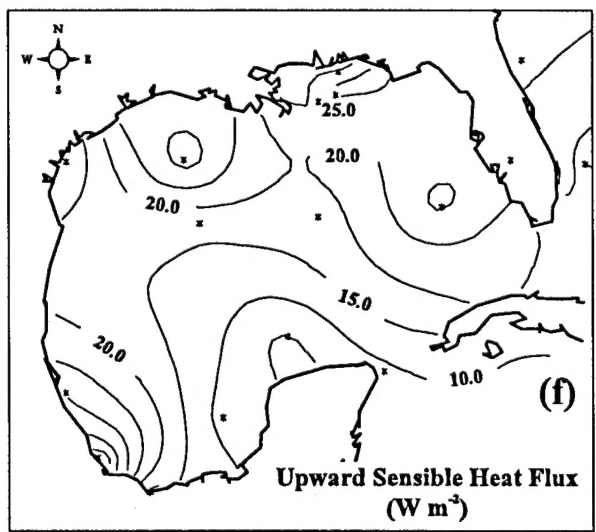
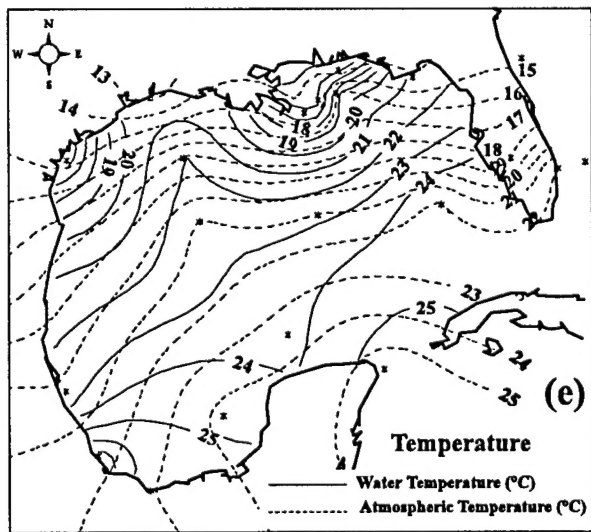
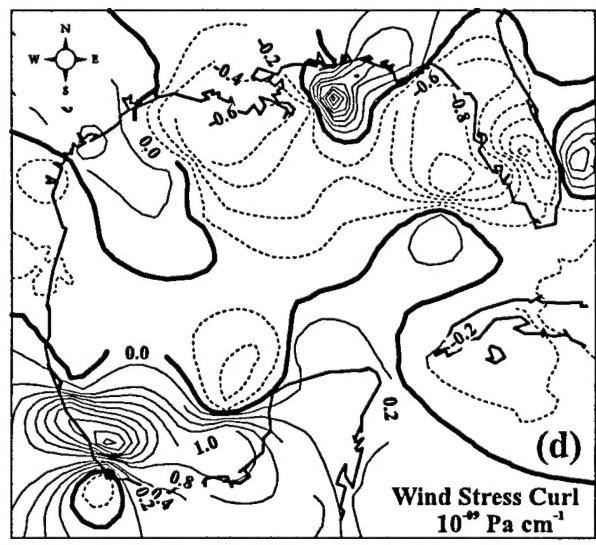
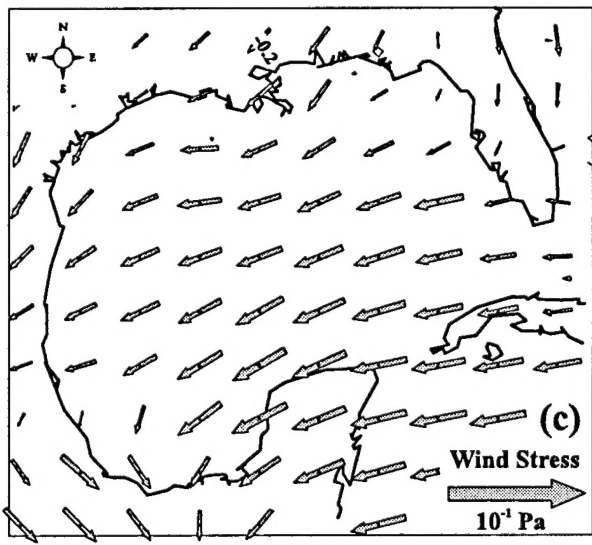
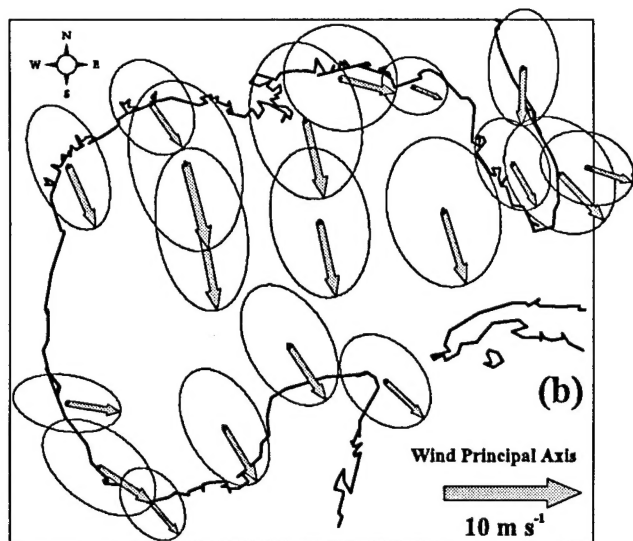
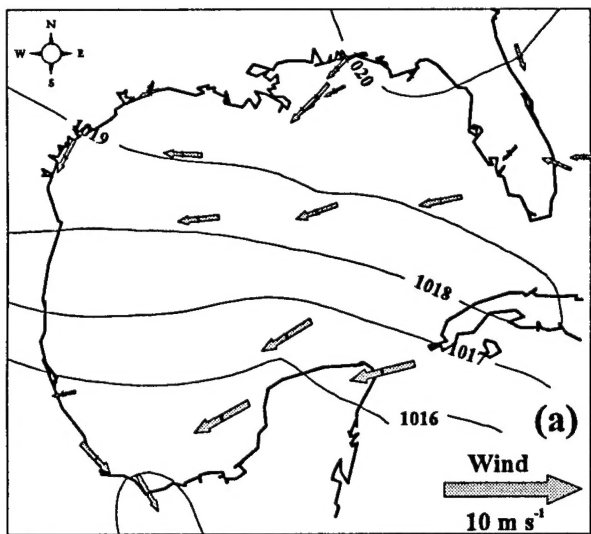


Fig 8